



Force detection of high-frequency electron spin resonance near room temperature using high-power millimeter-wave source gyrotron

Takahashi, Hideyuki ; Ishikawa, Yuya ; Okamoto, Tsubasa ; Hachiya, Daiki ; Dono, Kazuki ; Hayashi, Kanata ; Asano, Takayuki ; Mitsudo, ...

(Citation)

Applied Physics Letters, 118(2):022407

(Issue Date)

2021-01-11

(Resource Type)

journal article

(Version)

Version of Record

(Rights)

© 2021 Author(s). This article may be downloaded for personal use only. Any other use requires prior permission of the author and AIP Publishing. This article appeared in Applied Physics Letters 118, 2, 022407 (2021) and may be found at at <https://doi.org/10.1063/5.0036800>

(URL)


<https://hdl.handle.net/20.500.14094/90008682>



Force detection of high-frequency electron spin resonance near room temperature using high-power millimeter-wave source gyrotron

Cite as: Appl. Phys. Lett. **118**, 022407 (2021); <https://doi.org/10.1063/5.0036800>

Submitted: 08 November 2020 . Accepted: 29 December 2020 . Published Online: 13 January 2021

 Hideyuki Takahashi, Yuya Ishikawa,  Tsubasa Okamoto, Daiki Hachiya, Kazuki Dono, Kanata Hayashi, Takayuki Asano, Seitaro Mitsudo,  Eiji Ohmichi, and  Hitoshi Ohta



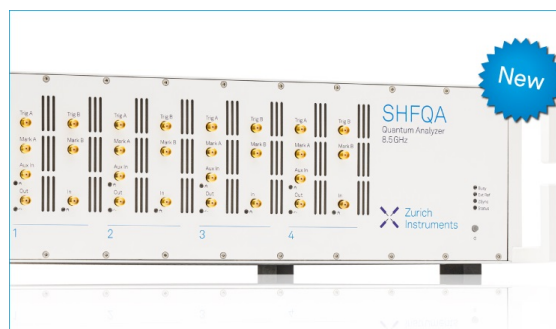
View Online



Export Citation



CrossMark



Your Qubits. Measured.

Meet the next generation of quantum analyzers

- Readout for up to 64 qubits
- Operation at up to 8.5 GHz, mixer-calibration-free
- Signal optimization with minimal latency

Find out more

 Zurich Instruments

Force detection of high-frequency electron spin resonance near room temperature using high-power millimeter-wave source gyrotron

Cite as: Appl. Phys. Lett. **118**, 022407 (2021); doi: [10.1063/5.0036800](https://doi.org/10.1063/5.0036800)

Submitted: 8 November 2020 · Accepted: 29 December 2020 ·

Published Online: 13 January 2021



View Online



Export Citation



CrossMark

Hideyuki Takahashi,^{1,a)} Yuya Ishikawa,² Tsubasa Okamoto,³ Daiki Hachiya,³ Kazuki Dono,² Kanata Hayashi,² Takayuki Asano,⁴ Seitaro Mitsudo,² Eiji Ohmichi,³ and Hitoshi Ohta¹

AFFILIATIONS

¹Molecular Photoscience Research Center, Kobe University, 1-1 Rokkodai-cho, Nada, Kobe 657-8501, Japan

²Research Center for Development of Far-Infrared Region, University of Fukui, Bunkyo 3-9-1, Fukui 910-8507, Japan

³Graduate School of Science, Kobe University, 1-1 Rokkodai-cho, Nada, Kobe 657-8501, Japan

⁴Department of Applied Physics, University of Fukui, Bunkyo 3-9-1, Fukui 910-8507, Japan

^{a)}Author to whom correspondence should be addressed: hide.takahashi@crystal.kobe-u.ac.jp

ABSTRACT

We report the measurement of force-detected electron spin resonance (FDESER) at 154 GHz using a gyrotron. The high output power allows the use of a strong transverse magnetic field larger than 10^{-4} T, which is sufficient to cause ESR saturation. We obtained the FDESER signal with a high spin sensitivity on the order of 10^{12} spins/G at 280 K. Our system has promising applications in high-frequency ESR studies of low-spin concentration samples, such as metalloprotein solutions.

Published under license by AIP Publishing. <https://doi.org/10.1063/5.0036800>

While commercial X-, Q-, and W-band electron spin resonance (ESR) spectrometers are used in various fields of science,¹ there is continuing demand for the development of ESR spectroscopy in higher field and frequency ranges. In the study of quantum magnets and metalloproteins, it is often critically important to observe ESR transitions across the large zero-field gap.² Conventionally, ESR spectroscopy above 90 GHz, so-called high-frequency ESR (HFESR),³ has been performed using the nonresonant transmission method.⁴ This technique covers a wide frequency range. However, it requires large samples, typically millimeter size or larger, due to its low sensitivity.

Force-detected ESR (FDESER) has been proposed as an alternative method.^{5–8} In FDESER, a slight change in the sample magnetization M_0 along with ESR absorption is detected after being converted into the magnetic gradient force F_{grad} . Owing to the high force sensitivity of micromechanical devices, the spin sensitivity is generally much higher than that of the transmission method. In our previous study, we achieved a sensitivity as high as 10^{12} spins/G at 1.6 K using a silicon nitride nanomembrane.⁹ This technique achieved precise broadband spectroscopy of submillimeter-sized samples and microliter solution samples.¹⁰ However, the ESR signal becomes smaller as the temperature increases, which hinders the practical application of this method.

The bottleneck in sensitivity improvement is evident in the magnetization change mechanism in ESR. The most common mechanism is the nonequilibrium process in which the spin-flip transition of electrons changes the occupancy of different spin states. This change can be obtained by solving Bloch's equation, which is given as

$$\Delta M_z^{\text{Bloch}} = -M_0 \frac{\gamma^2 B_1^2 T_1 T_2}{1 + \gamma^2 B_1^2 T_1 T_2}, \quad (1)$$

where B_1 , γ , and T_1 and T_2 are the transverse magnetic field of the electromagnetic wave, gyromagnetic ratio, and spin-lattice and spin-spin relaxation time, respectively.¹¹ In a typical case, $|\Delta M_z^{\text{Bloch}}/M_0| \ll 1$ in the high-frequency region owing to the low power of the millimeter/terahertz wave source. Even for 2,2-diphenyl-1-picrylhydrazyl (DPPH) with a relatively long $T_1 = 77$ ns and $T_2 = 64$ ns,¹² $|\Delta M_z^{\text{Bloch}}/M_0|$ is estimated to be $\sim 1 \times 10^{-4}$ with a typical value of $B_1 \sim 10^{-6}$ T for a 10 mW class millimeter-wave source in combination with an oversized circular waveguide. The other mechanism is much simpler and is due to heating by ESR.⁹ The energy absorbed by ESR is used to increase the sample temperature in the spin-lattice relaxation process. By irradiating the slowly amplitude-modulated

millimeter wave, $M_0(T)$ can be modulated while maintaining thermal equilibrium. The amplitude modulation is given as $\Delta M_z^{th} = \frac{\alpha}{C} \left| \frac{dM}{dT} \right|$, where C is the heat capacity of the sample and α is the coefficient that depends on experimental parameters, such as millimeter-wave power and modulation frequency. It is important to note that ΔM_z^{th} does not depend on T_1 and T_2 . However, it is difficult to observe the signal at high temperatures because of the decreasing dM/dT and increasing C .

Regardless of the mechanism used, a high-intensity electromagnetic wave source is expected to fundamentally solve the sensitivity problem. In this Letter, we report FDESER spectroscopy using a millimeter-wave gyrotron. Its high output power enables us to observe the FDESER signal even at room temperature while maintaining the spin sensitivity of 10^{12} spins/G.

A gyrotron is a vacuum tube oscillator that generates high-power millimeter waves by the cyclotron resonance of electrons inside the cavity placed in a magnetic field. In this study, we used the 154 GHz gyrotron FU CW VII B developed at the University of Fukui. It has a frequency stability of ± 2 MHz, and other output characteristics are also optimized for spectroscopic studies. For the details of FU CW II B, refer to the review paper in Ref. 13.

Figure 1(a) shows the schematic of the gyrotron FDESER system. FU CW II B was operated in the pulse mode with a repetition of 5 Hz and a duty ratio of $D = 0.1\%$ – 10% . The peak and average power of the millimeter wave in the sample space were estimated to be $P_{\text{peak}} = 5$ W

and $P_{\text{av}} = P_{\text{peak}}D = 5$ – 500 mW, respectively. The millimeter-wave beam has a rather complex spatial profile immediately after exiting the gyrotron, reflecting the electromagnetic field distribution in the cavity. For the transmission efficiency, the millimeter-wave beam was shaped by the mode converter so that it has a Gaussian spatial distribution.¹⁴ Afterward, it was transmitted through the quasi-optical mirror system (the details of this system will appear elsewhere) into a gas flow-type cryostat inserted into a superconducting magnet. Although the mirror configuration was optimally designed for pulsed ESR spectroscopy,¹⁵ it can also be applied to continuous-wave ESR experiments. After entering the polytetrafluoroethylene window at the top of the cryostat, the millimeter wave propagated inside the 1-m-long circular corrugated waveguide to the sample space. B_1 in the sample space was estimated to be $B_1 = 1.9 \times 10^{-4}$ T from the pulsed-ESR measurement.

Figure 1(b) shows the schematic of the ESR probehead. All the body parts were made of nonmagnetic brass. A ferromagnetic particle with a diameter of $40 \mu\text{m}$ was glued to the center of the 100-nm-thick silicon nitride membrane (MEMN03001/7.5M, NTT Advanced Technologies Corporation) using a small amount of Stycast 1266 epoxy. The membrane was embedded into the brass block and covered by the CuBe plate with a spacing of $100 \mu\text{m}$, on which the sample was placed. The magnetic field gradient generated by the magnetic particle was calculated using the magnetic dipole model. Using the magnetic moment of the probe magnet of $m_z = 9.1 \text{ A/m}^2$ and the distance

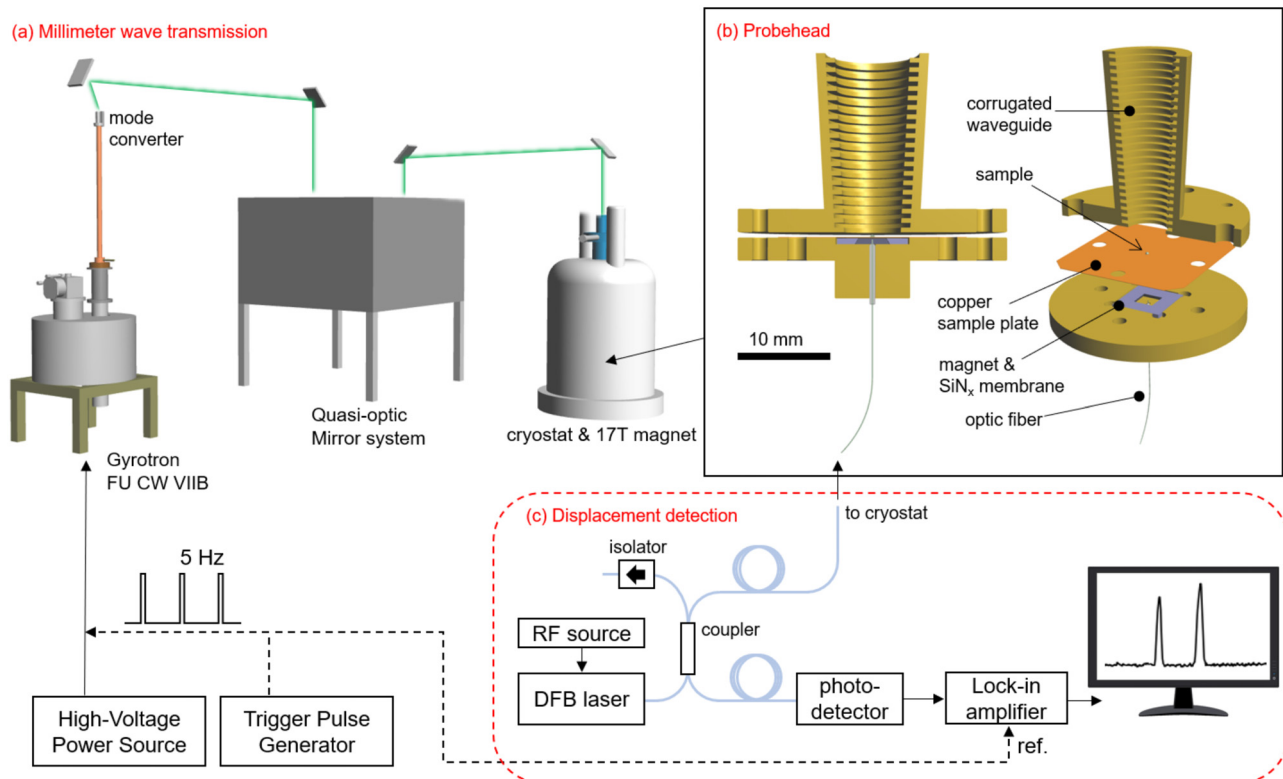


FIG. 1. (a) Schematic of the gyrotron FDESER system. (b) Cross-sectional view of the FDESER probehead and part configuration. (c) Setup of optical interferometry for the displacement detection of the nanomembrane.

between the sample and the probe magnet of $h = 0.17$ mm, the magnetic field gradient is estimated to be $G_z = \frac{3\mu_0 m_z}{2\pi h^3} = 6.5$ T/m at the sample position.

When the ESR condition was satisfied, the change in F_{grad} between the sample and the probe magnet displaced the membrane. This displacement was measured by optical interferometry. The configuration of the fiber-optic interferometer is basically the same as that in Refs. 7 and 16, except that we used the distributed feedback (DFB) laser (LP1550SAD2, Thorlabs) instead of the wavelength-tunable laser to reduce costs [Fig. 1(c)]. Although the DFB laser is designed for single-frequency operation, its wavelength can be tuned by approximately 2 nm by adjusting the device temperature. The coherence length of the DFB laser is so large that unwanted interference (inside the fiber between the connectors) caused issues in measuring the device displacement. For this reason, we superimposed an RF (10–20 MHz) current on the DC bias current and degraded the coherence. The amplitude of the membrane vibration was measured using the lock-in amplifier with a time constant of 1 s.

For the test samples, we used 20 μg of DPPH powder and a single $\text{Cu}(\text{C}_4\text{H}_4\text{N}_2)(\text{NO}_3)_2$ (CuPzN) crystal with dimensions of $0.8 \times 0.5 \times 0.08$ mm³. DPPH is an organic free radical compound that is widely used as an ESR standard. CuPzN is a one-dimensional quantum spin chain material with a very low Neel temperature of $T_N = 107$ mK.^{17,18} It has two inequivalent Cu^{2+} ($S = 1/2$) ion sites whose principal axes are in different directions. We applied the magnetic field in the [010] direction, which corresponds to the bisector of these principal axes. In this case, a single Lorentzian-type absorption line is expected to be observed at the magnetic field corresponding to $g = 2.26$.¹⁹

Figures 2(a) and 2(b) show the FDESER spectra of DPPH powder at $T = 10$ and 50 K. At low temperatures, the temperature of the sample space increased because of the high-power millimeter waves. To avoid this problem, measurements at 10 K were performed at $D \leq 1\%$. We observed the peak signal at the magnetic field corresponding to the g -factor of DPPH ($g = 2.0036$). The obtained linewidths are $\delta B = 1.5$ – 2.5 mT, which is broader than the intrinsic value.²⁰ In general, the FDESER spectrum is somewhat distorted because the sample was placed in a nonhomogeneous magnetic field. Since the linewidth of DPPH powder depends on the amount of

adsorbed oxygen, it is difficult to evaluate the linewidth broadening accurately. Nevertheless, considering $G_z = 6.5$ T/m and the thickness of the sample (50–100 μm), broadening of a few Gauss is inevitable.^{20,21} There are other minor factors that affect the accuracy of g -factor determination, such as the magnetic field sweep rate, the lock-in time constant, and the gyrotron frequency stability. Therefore, samples with narrow linewidths need to be measured carefully. On the other hand, these errors are not an issue in the analysis of signals from magnetic ions, which are the main target of HFESR.

The ESR signal increased with increasing D . At the same time, we found the increasing offset signal. The offset component is often observed in FDESER experiments and is referred to as spurious oscillation.²² Its effect is particularly serious when the micromechanical device is directly exposed to an amplitude-modulated electromagnetic wave. In our setup, the spurious oscillation was effectively reduced by the shielding structure around the membrane. However, the periodic Joule heating of the probehead parts could indirectly cause a change in F_{grad} . For example, the millimeter wave heats only the upper part of the sample plate and causes thermal distortion, which vertically deflects the sample plate. Consequently, the magnetic field gradient at the sample position is modulated, which causes spurious oscillation of the membrane.

We extended the measurement to the room temperature region ($T = 280$ K), as shown in Fig. 3(a). This result shows the advantage of the high-power millimeter-wave source. The performance of our system was also demonstrated by the measurement of CuPzN single crystals with a broader linewidth than DPPH [Fig. 3(b)]. The baseline at 280 K was found to have a linear slope, which is related to the thermal drift of the interferometer tuning. Since the drift rate is nearly constant for short time measurements, it can be removed by assuming a linear baseline. The feedback control of the cavity length will be more useful for removing the thermal drift, which was not implemented in our current setup.²³

To quantitatively evaluate the sensitivity, we use the absolute spin sensitivity $S = N_{\text{spin}}/(\eta\delta B)$, where N_{spin} and η are the total spin number and signal-to-noise ratio, respectively. This value represents the number of spins per 1 G of spectral width that can be detected with a signal-to-noise ratio of 1. Figure 4 shows the

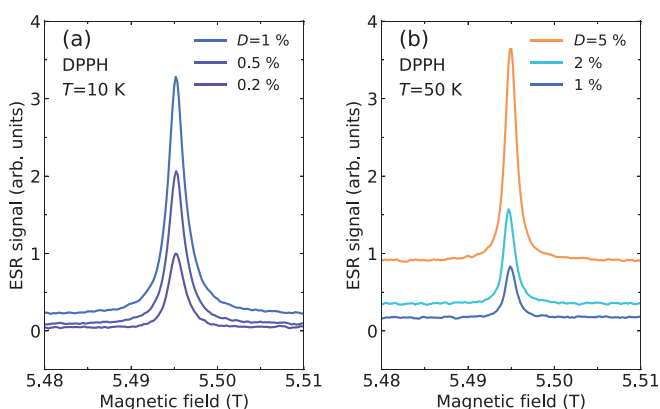


FIG. 2. FDESER spectra of DPPH powder with different duty ratios at (a) $T = 10$ K and (b) $T = 50$ K. The magnetic field was swept at a rate of 10 mT/min.

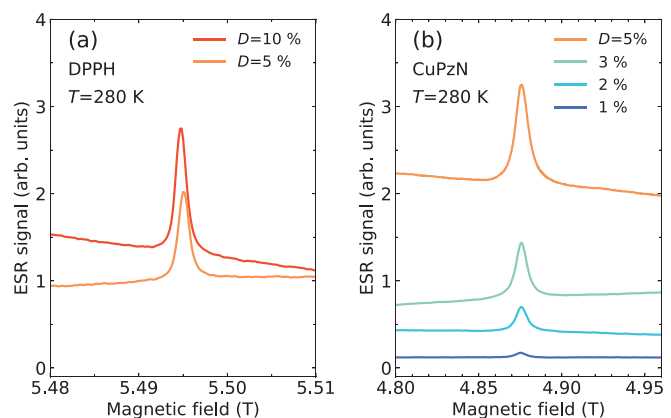


FIG. 3. FDESER spectra of (a) DPPH powder and (b) CuPzN single crystal with different duty ratios at $T = 280$ K. The magnetic field sweep rates are 10 mT/min in (a) and 20 mT/min in (b).

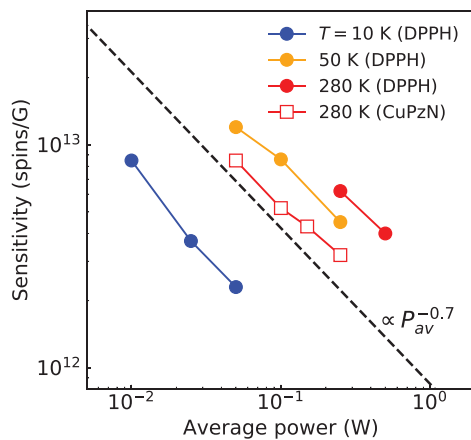


FIG. 4. Average power dependence of the spin sensitivity. The dashed line shows the slope of $P_{av}^{-0.7}$.

P_{av} dependence of S . It is noteworthy that we achieved a high spin sensitivity on the order of 10^{12} – 10^{13} spins/G over the entire temperature range. The small temperature dependence of S indicates that $|\Delta M_z^{\text{Bloch}}| \gg |\Delta M_z^{\text{th}}|$ under the current experimental condition. As previously mentioned, although the detection of ΔM_z^{th} is very effective at low temperatures, the sensitivity drastically decreased as T increased.⁹ Considering the temperature dependence of $dM_0/dT (\propto T^{-2})$ and C , ΔM_z^{th} at $T = 50$ K is expected to be less than that at $T = 10$ K by two orders and even lower at 280 K. On the other hand, $|\Delta M_z^{\text{Bloch}}/M_0|$, which was very small with a low power source, was enhanced by the large B_1 value of the gyrotron. Because $\gamma^2 B_1^2 T_1 T_2$ for DPPH is an order of unity even at room temperature, $\Delta M_z^{\text{Bloch}}$ exhibits a similar temperature dependence on M_0 , which obeys the Curie law $M_0 \propto T^{-1}$.

The noise amplitude in the spectrum corresponds to the vibration noise amplitude of 30–100 pm. This value is much larger than the thermal oscillation noise of 1–10 pm expected from the equipartition theorem, indicating that there is room for noise reduction. The largest source of noise is likely to be the flow of helium gas in the cryostat. Although the gas flow does not directly touch the device, this type of cryostat is generally not suitable for displacement measurements. We also observed the influence of spurious noise on the power dependence of spin sensitivity. The increase in S was not directly proportional to P_{av} but was roughly proportional to $P_{av}^{0.7}$. This is attributed to the fact that spurious noise tends to be larger on the high D side. Several noise reduction schemes are expected to make this method more practical in the measurement of low-spin concentration samples, for example, the use of the liquid ^4He bath-type cryostat, thermal design of probes to reduce spurious noise, and general vibration isolation techniques.

Some studies have used a gyrotron for transmission-type ESR.²⁴ However, sensitivity did not improve as expected from the high millimeter-wave intensity. In the transmission method, the high-power millimeter wave increased not only the ESR absorption but also the background signal. Therefore, the gain of the detection system should be reduced to avoid pre-amplifier saturation. On

the other hand, the force detection system did not return the signal unless the ESR condition was satisfied, apart from the spurious signal discussed above. Since the millimeter-wave intensity can be increased without reducing the detection gain, the sensitivity improvement is more straightforward than that of the transmission-type ESR.

In conclusion, we developed an FDESr spectroscopy technique using a 154 GHz gyrotron. We obtained the ESR signal of DPPH and CuPzN in the room temperature region with a spin sensitivity on the order of 10^{12} spins/G. This method does not have limitations in terms of the electromagnetic wave frequency. The combination with a multi-frequency gyrotron, which can generate multiple frequencies by selectively exciting the higher-order cyclotron modes inside the cavity, is a promising method to broaden the frequency range.²⁵ Force detection can also be combined with other high-power electromagnetic wave sources, such as free electron lasers.^{26,27}

This study was partially supported by the Murata Science Foundation.

DATA AVAILABILITY

The data that support the findings of this study are available from the corresponding author upon reasonable request.

REFERENCES

- C. P. Poole, Jr., *Electron Spin Resonance*, 2nd ed. (Dover, New York, 1996).
- H. Ohta, S. Okubo, K. Kawakami, D. Fukuoka, Y. Inagaki, T. Kunimoto, and Z. Hiroi, *J. Phys. Soc. Jpn.* **72**(Suppl. B), 26 (2003).
- S. S. Eaton and G. R. Eaton, "Chapter XI: High magnetic fields and high frequencies," *Handbook of Electron Spin Resonance* (Springer-Verlag, New York, 1999), Vol. 2, pp. 345–370.
- M. Motokawa, H. Ohta, and N. Maki, *Int. J. Infrared Millimeter Waves* **12**, 149 (1991).
- D. Rugar, C. S. Yannoni, and J. A. Sidles, *Nature* **360**, 563 (1992).
- H. Takahashi, E. Ohmichi, and H. Ohta, *Appl. Phys. Lett.* **107**, 182405 (2015).
- E. Ohmichi, Y. Tokuda, R. Tabuse, D. Tsubokura, T. Okamoto, and H. Ohta, *Rev. Sci. Instrum.* **87**, 073904 (2016).
- E. Ohmichi, T. Okamoto, H. Takahashi *et al.*, *Appl. Magn. Reson.* (published online 2020).
- H. Takahashi, T. Okamoto, K. Ishimura, S. Hara, E. Ohmichi, and H. Ohta, *Rev. Sci. Instrum.* **89**, 083905 (2018).
- T. Okamoto, H. Takahashi, E. Ohmichi, H. Ishikawa, Y. Mizutani, and H. Ohta, *Appl. Phys. Lett.* **113**, 223702 (2018).
- A. Abragam and B. Bleaney, *Electron Paramagnetic Resonance of Transition Ions* (Clarendon Press, Oxford, 1970).
- Krishnaji and B. N. Misra, *Phys. Rev.* **135**, A1068 (1964).
- T. Idehara and S. P. Sabchevski, *J. Infrared, Millimeter, Terahertz Waves* **38**, 62 (2017).
- S. N. Vlasov and I. M. Orlova, *Radiophys. Quantum Electron.* **17**, 115 (1974).
- S. Mitsudo, K. Kono, K. Dono, K. Hayashi, Y. Ishikawa, and Y. Fujii, in 2019 44th International Conference on Infrared, Millimeter, and Terahertz Waves (IRMMW-THz), Paris, France (2019), p. 1.
- D. T. Smith, J. R. Pratt, and L. P. Howard, *Rev. Sci. Instrum.* **80**, 035105 (2009).
- A. Santoro, A. D. Mighell, and C. W. Reimann, *Acta. Crystallogr. Sect. B* **26**, 979 (1970).
- T. Lancaster, S. J. Blundell, M. L. Brooks, P. J. Baker, F. L. Pratt, J. L. Manson, C. P. Landee, and C. Baines, *Phys. Rev. B* **73**, 020410(R) (2006).
- A. A. Validov, M. Ozerov, J. Wosnitza, S. A. Zvyagin, M. M. Turnbull, C. P. Landee, and G. B. Teitelbaum, *J. Phys.: Condens. Matter* **26**, 026003 (2014).
- N. D. Yordanov, *Appl. Magn. Reson.* **10**, 339 (1996).

- ²¹N. S. Garif'yanov and B. M. Kozyrev, Dokl. Akad. Nauk SSSR **118**, 738 (1958).
- ²²K. J. Bruland, J. Krzystek, J. L. Garbini, and J. A. Sidles, *Rev. Sci. Instrum.* **66**, 2853 (1995).
- ²³H. Takahashi, T. Okamoto, E. Ohmichi, and H. Ohta, *Appl. Phys. Express* **9**, 126701 (2016).
- ²⁴T. Tatsukawa, T. Maeda, H. Sasai, T. Idehara, M. Mekata, T. Saito, and T. Kanemaki, *Int. J. Infrared Millimeter Waves* **16**, 293 (1995).
- ²⁵Y. Tatematsu, Y. Yamaguchi, R. Ichioka, M. Kotera, T. Saito, and T. Idehara, *J. Infrared, Millimeter, Terahertz Waves* **36**, 697 (2015).
- ²⁶S. A. Zvyagin, M. Ozerov, E. Cizmar, D. Kamenskyi, S. Zherlitsyn, T. Herrmannsdorfer, J. Wosnitza, R. Wunsch, and W. Seidel, *Rev. Sci. Instrum.* **80**, 073102 (2009).
- ²⁷S. Takahashi, L.-C. Brunel, D. T. Edwards, J. van Tol, G. Ramian, S. Han, and M. S. Sherwin, *Nature* **489**, 409 (2012).